Journal of Engg. Research **Vol. 3 No. (1) Mar 2015** pp. 51-77

التحقق من تدفق في السد الجانبي على طول قناة منحنية

***م. أوزتورك ، **أ. يوسيل و ***م . س . التونة**

* أستاذ مشارك ، جامعة فرات، قسم الهندسة المدنية، إيلازيغ، تركيا

** مدرس، جامعة كوكوروفا، قسم تكلونوجيا الهندسة المدنية، أضنة، تركيا

*** أستاذ مساعد، جامعة فرات، قسم الهندسة المدنية، إيلازيغ، تركيا

الخلاصة

تستخدم السدود الجانبية في الري ومجال الصرف وشبكات الصرف الصحي وقنوات بجانب السدود والأحواض اللازمة لصرف الفائض دون الأضرار بالبيئة. وفي هذه الدراسة، يتم استخدام أنبوب الرى الذاتي بدلا من الجانبي الهدار لعدد من الزوايا (300، 600 و 900) من قناة منحنية ومسطحة ، وتم قياس مستوى الماء وسرعتها من خلال فتح وإغلاق بوابة مستوى التنظيم في تصريف وبمستويات مختلفة. ونتيجة هذه القياسات، تم تحديد متوسط مستوى سطح الماء وعرضها في صور. أرقام فرويد ومعامل حساب التصريف والتفريغ تم حسابها وبالإضافة إلى ذلك، تم التحقق من التدفق الحلزوني.

The investigation of side-weir siphons flow along a curved channel

M. Öztürk*, A. Yücel** and M.C. Tuna***

**Firat University, Civil Engineering Department, 23119, Elazig, Turkey*

Email:mozturk1@firat.edu.tr

*** Instructure Dr., Cukurova University, Civil Engineering Technician Department, 01160, Adana, Turkey Email: ahmetyucel@cu.edu.tr*

****Firat University, Civil Engineering Department, 23119, Elazig, Turkey*

Email:cihattuna@gmail.com

ABSTRACT

Side weirs are being used commonly in irrigation, field drainage, sewage systems, side channel spillway dams and settling basins to supply needed discharge or put away excess discharge without giving harm to the environment. In this study, self-priming siphon was used instead of side weir. Settled in the different angels (30^0, 60^0 and 90^0) of a curved channel and flat side (0^0), water level and velocity were measured by opening and closing of the regulating level gate in different discharges and levels. At the result of these measurements, water surface profiles and depth averaged velocities were found and shown in figures. Froude numbers, siphon spillway discharge and discharge coefficients were calculated. In addition, siphon spillway and priming, depriming and helicoidal flow were investigated.

Keywords: Depth averaged velocities; Priming and depriming; Side weir; Siphon spillway; Water surface profiles

INTRODUCTION

Side-weirs, also known as lateral weirs, are widely used in irrigation, land drainage, urban sewage systems by flow diversion or intake devices. Irrigation is being projected according to optimum capacity by considering the needs and economy of the transfer waterways intended for water supply of hydroelectric and other hydraulic structures. In order to avoid flood of excess water entered into waterway, side weirs are being made where necessary. These weirs are called as side weirs since they are being attached on one or both sides of the waterway or on sides of facilities like sedimentation tank. Side weirs are used quite often in combined sewer systems in residential areas.

Side weir term which is used to remove water from the waterway or a reservoir is being used in two types of hydraulic structures. The first among these is the classic side

weir. Classical side weirs are being used in order to achieve a certain level of water or to remove a certain portion of the flow. The second one is spillways. Spillways are being used for the removal of flood flow from the reservoirs. These are: free surface spillways, covered free surface weirs, shaft (well) weirs and siphon weirs. Siphon weirs have many advantages over free surface weirs and they have a wide usage area as spillway.

Side weir crest is generally placed parallel to waterway axis or as to make a specific angle. Generally rectangular, triangular or trapezoidal cross-sections are used as side weirs. Due to the lateral stream, flow structure between the weir and main waterway shows a gradually varied character. Accurate detection of spill flow amount is theoretically very difficult. Therefore, experimental studies are preferred for better detection of flow conditions.

The velocity distributions generally depend on the waterway cross-section type. Although researchers studied on trapezoidal, semi-circular, etc. waterway cross-sections, there are no studies in the literature about side weirs placed in sinuous waterways work, and about usage of siphons at sinuous waterways as side weirs.

In this study, curved free surface is used as outdoor plant level control channels instead of the classic side spillways, due to the known advantages of the side of the siphon valves used. Thus, in cases where the length of the weir is limited, it will be possible for siphon to keep the water level in the desired value by applying the side weirs. In addition, in case of formation to get water, it will be possible to take a desired certain amount of water from the waterway. Water levels, fluid flow, velocity distributions, flow rate of siphon weirs and working conditions are being investigated experimentally.

SUMMARY OF LITERATURE

Babaeyan-Koopaei et.al (2001 & 2002) studied on physical models about siphon models in order to drain excess water safely from the barrage which was built in 1930 in the UK.

Hardwick & Grant (1997) studied on air-regulated siphon weirs so as to be used in Pargau hydroelectric project.

Avcı (1975) conducted studies on the classic and automatic siphon weirs. In these studies, he examined the streams by placing the classic and automatic siphons over straight waterways as spillways and side weirs.

Some researchers (Khatsuria , 2005); Erkek & Ağiroğlu (2002); Davies (1931); Inglis (1931); Gibson , Aspey & Tattersal (1930) monitored that reverse flow and stagnation occurred in the downstream of the side weirs in their experimental studies

conducted in river regime flow conditions. According to these researchers, the location and length of separation zone depends on the Froude number at the side weir upstream and on the length of the side weir. In addition, El-Khashab (1975) indicated the kinetic energy of the flow in the main waterway decreased due to the spill, while moving downstream along the side weir (Froude number decreases along the side weir), secondary flow aroused from side flow intensified along the side weir, and existence of separation zone at the end of the first half of the side weir and reverse flow in the second half.

Shukry (1950) experimentally investigated the amount of bulking that occurred at the sinuosity and maximum speed orbit at the sinuosity. He used a term known as the power of helical movement in order to express the effect and the magnitude of helical flow in various sinuosities of various flow conditions. This statement is being described as the ratio of the average kinetic energy of a secondary movement in a given cross-section to the total kinetic energy of the flow. El-Khashab (1975) indicated that intensity of the secondary flow occurred due to lateral spill in the linear waterway is similar to the one at the sinuosity.

Choudhary & Narasimhan (1977) indicated that helical movement at the 180° open waterway sinuosity in a river regimes flow conditions is begun at the outer coast in $\theta=150^0$ and reached the maximum at $\theta = 135°$ in outer coastal region, and large shear stresses occurred. Ağaççıoğlu & Yüksel (1998) stated in their studies about side weir flow, which is placed along a outer part of the curved waterway that the maximum speed orbital is placed; at the main waterway in the linear approach waterway, after the curve inlet at the inner shore at $\theta = 30°$, after $\theta = 30°$ at the outer shore at the $\theta = 60°$ and remain there till $\theta = 120º$ and then returned to the waterway axis again. The researcher stated that the direction of the speed orbital is close to lateral flow around $\Theta = 30 °$.

Neary& Odgaard (1993) experimentally studied the three-dimensional flow structure at the $\theta = 90^o$ open waterway branch (separation) and reported that they showed characteristics similar to flow structure at the stream sinuosity. They have stated that the behavior of the three-dimensional flow depends on the roughness of the main waterway and on the ratio of lateral flow speed to speed of main waterway (spill ratio).

Gibson , Aspey & Tattersal (193 0) experimentally studied on Siphon Spillways, and developed their formula, $d\sqrt{h} > 47.1\ cm^{3/2}$.

DETERMINATION OF EFFECTIVE PARAMETERS IN AN EXPERIMENTAL STUDY

There are many parameters affecting the side weir flow which are listed in Table 1.

Table 1. The parameters that affect the side weir flow

Name	Sign	Unit	Size
The main waterway width	B	m	L
Curvature radius	r	m	L
Curve centre angle	θ	--	--
Waterway base slope	J_0	--	--
Waterway roughness	n	--	--
Specific mass of the fluid	ρ	kg/m^3	ML^3
Dynamic viscosity of the fluid	μ	kg/m.s	$ML^{-1}T^{-1}$
Acceleration of gravity	g	m / s^2	LT^{-2}
Surface tension	N / m^2	K	L^{-2}
Flow depth	h	m	L
The average flow speed changing along the side weir	V	m / s	LT^{-1}
Deflection angle of the flow effecting the side weir	α	--	--
The weir width of the siphon	b	m	L
The height of the siphon	d	m	L
Siphon bend angle	R_0	--	--

DIMENTIONAL ANALYSIS

Side weir flow rate coefficient C_d is the function of the following parameters:

$$f(C_d, B, r, \theta, J_0, n, \rho, \mu, g, \sigma, h, V, \alpha, R_0, b, d) = 0 \quad (4.2)$$

Since the effect of J_0, n, σ, μ and ρ are insignificant for a elementary flow particle, they can be neglected, El-Khashab (1975). Therefore;

It can be written in the form of:

$$f(C_d, B, r, \theta, g, h, V, \alpha, R_0, b, d) = 0 \quad (4.3)$$

Table 2. Dimension analysis for the parameters that affect the side weir coefficient

	K_1	K_2	K_3	K_4	K_5	K_6	K_7	K_8	K_9	K_{10}	K_{11}
	B	V	b	d	α	r	θ	C_d	g	h	R_0
L	1	1	1	1	0	1	0	0	1	1	0
M	0	0	0	0	0	0	0	0	0	0	0
T	0	-1	0	0	0	0	0	0	-2	0	0

In this case, M seems to be in just a single parameter. Therefore, the flow is kinematics. Repeated magnitudes are taken as g and h.

In that case, among these dimensionless quantities;

$C_d = f(Fr, \frac{b}{B}, \frac{b}{r}, \frac{d}{h}, \alpha, \theta, R_0)$ is obtained.

since $\frac{b}{B}$ = constant and R_0 = is fixed,

It can be written as $C_d = f(Fr, \frac{b}{r}, \frac{d}{h}, \theta)$ (4.4)

Fr is the Froude number which is found according to the depth of water measured in the waterway axis at the beginning of the side weir.

Due to lack of oscillations in the main waterway and the existing tools, C_d is considered as the Froude number effecting the side weir flow rate coefficient and the Froude number which is found according to the h water level at the side weir upstream in the waterway axis was taken into account. In reality however, due to lateral flow along the side weir, Froude number is changeable Agaccioglu & Yuksel (1998). Therefore, effect of the angle deviation which the Froude number (changing throughout the side weir) has an impact on was not taken into account.

MATERIALS AND METHODS

In this study, the experimental study is conducted at the 180 sinuous waterway existed in the Firat University Faculty of Engineering Department Civil Engineering Hydraulic Laboratory. This sinuous waterway in Figure 1 consists of 50cm wide and 50cm height main waterway and collecting waterway of same dimensions (also extensions in the form of half circles exist in front of the weirs). Test waterway parts include:

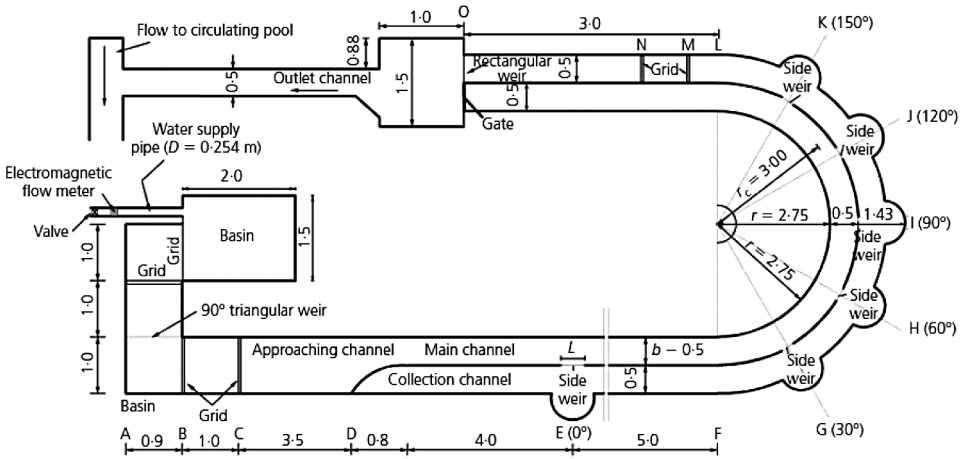

Fig. 1. Experimental setup (dimensions given in m)

Home depot

The water in the main depot at the basement is being pumped to depots at the upper floors with 3 pumps and the desired amount of water is being sent to test waterway with a pipe from the depot from here. Before entering into stilling pool which feed the test waterway, flow of the incoming water is being adjusted by electromagnetic flow meter.

Stilling pool feeding the test waterway and triangular weir

Stilling pool feeding the waterway is of size of 2 m x 1, 5 m and 0, 9 m x 2 m (L-shaped) and 0,7m height. Water-hole grids are placed in the pool to cool down the water. There exists a triangle weir with 0.90m upper width at the end of the pool (Figure 2).

Fig. 2. Stilling Pool and Triangular Weir

Stilling pool after the weir

Water flowing through the triangular weir to waterway is being rested in a secondary stilling pool with dimensions of 0, 9 m x 0, 9 m. Sedatives are still available after this pool (Figure 2).

Test waterway:

Approach waterway

Approach waterway consists of 3.5m x 1m linear input channels and 1m transition waterway and 0,5 x 0, 5m cross-section linear main waterway. The outer parts of the approach waterway are made of glass. 4.5m after the stilling pool, there is a throttling in the waterway. After this throttling, the incoming water reaches a=0 weir at the approach waterway (flat portion) and then respectively reaches to $\alpha = 30^0$, $\alpha = 60^0$, $\alpha = 90^0$ $\alpha = 120^0$ and $\alpha = 150^0$ weirs at the sinuous parts.

Sinuous waterway

The curved waterway which is seen in the Figure 4 is a channel with the radius of axis r = 2.75m and curved at 180 ^{0} 'of. This waterway consists of the main and collecting waterways and semi-circular extensions were made for ease of water flow to the front of the weirs existing at the collecting waterways and in order to monitor the flows.

Collecting waterway

The water collected in the side weir was removed from the 0.50 m width collecting waterway. There is a rise difference of 20 cm between the collecting waterway and the main waterway. Again, in order to monitor the flow easily, the outer part of the waterway was made of Plexiglas. By placing a 0.5m width, 7.05 cm threshold height rectangular weir at the end of the collecting waterway, spill flow rate was being determined. An electronic limn meter was being used, which was placed at a distance of 95 cm from the weir (Figure 3).

Fig. 3. The general scheme of the experiment channel

Linear outlet waterway

A 2 piece water level adjust cap (Figure 4) is placed at the end of the 3.0 m length linear outlet waterway. The left side is collection channel and right side is main channel. Main channel waterway is higher than collection channel.

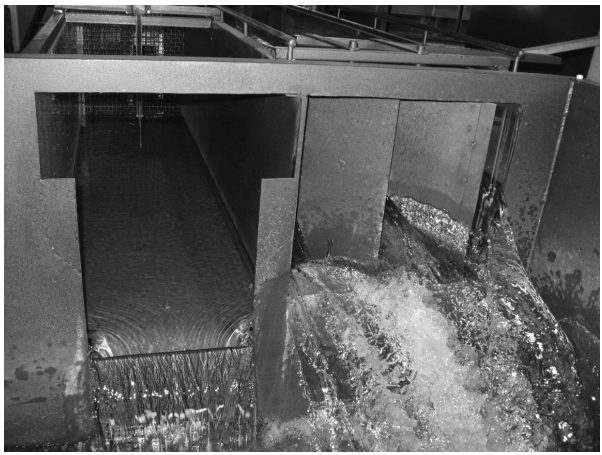

Fig. 4. Collecting Waterway

Side weir separation wall

Outer walls of the main waterway were made of transparent material (Plexiglas) in order to observe the flow. Glass was used in flat sections. The inner wall was made of sheet metal. Places of the side weirs were determined over the inner wall after the curve inlet, so as to see its side weir axis at the circle arcs of $30^{0,}$ $60^{0,}$ $90^{0,}$ $120^{0,}$ $150^{0,}$.

Collecting waterway

The water collected in the side weir was removed from the 0.50 m width collecting waterway. There is a rise difference of 20 cm between the collecting waterway and the main waterway. Again, in order to monitor the flow easily, the outer part of the waterway was made of Plexiglas. By placing a 0.5m width, 7.05 cm threshold height rectangular weir at the end of the collecting waterway, spill flow rate was being determined. An electronic limn meter was being used, which is placed at a distance of 95 cm from the weir (Figure 4).

Fig. 4. The general scheme of the experiment channel

Discharge (outlet) waterway

The flow which passed through the water level adjust cap of the main waterway and the collecting waterway was sent back to the main depot after pouring to discharge (outlet) waterway.

Moving, level and speed measurement car

Speed and level measurements were made with the help of a special designed car, which moved over the pipes at the main waterway. Speed and level measurement devices were mounted on this car and measurements were made (see Figure 5).

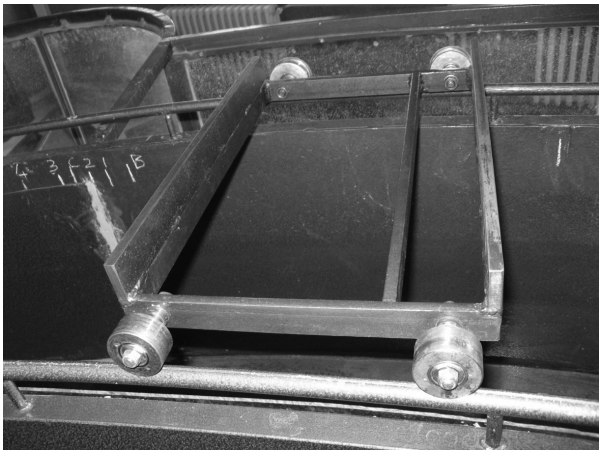

Fig.5. Moving, level and speed measurement car

Preparation of siphon model

Since a siphon model will work with a mixture of air and water, it is not possible to mention a complete similarity about whole phases of the flow. However, model experiments are considered to be the best guide for conceptualization of a siphon project.

The law of similarity which to be taken as a basis in Siphon models is determined by the value of the Reynolds number Wehry (1969). In general, Froude affinity is taken as a basis for the models which have Reynolds number bigger than $2 * 10^5$ and Reynolds affinity for the models have smaller Reynolds number than this value. This is because, at large Reynolds numbers, gravity forces are more effective compared to viscous forces whereas viscosity forces gain more importance at the Reynolds number smaller than the $2 * 10^5$.

The siphon used in the experiment is automatic priming siphon. This siphon is made of transparent material (Plexiglas) in order to monitor the flow. For details of siphon which was given in the figure, Gibson's minimum model scale conditions formula is $d\sqrt{h} > 47.1$ $cm^{3/2}$ is applied after wood moldings were prepared for the construction the siphon. After heating the lower and upper face plates (crest and top faces) of the siphon which was made by Plexiglas material in the drying-oven, they were placed into wood forms and required shapes were given. These profiles are being cut from flat Plexiglas plate and mounted on the leveled siphon side surfaces with a special Plexiglas adhesive and silicone.

This model seen in figure 6 is automatic priming and its inlet cross-section of roof-section is 12x18 cm, and it has a rectangular shaped section within 12x7 cm size from priming unit, which has originated after the roof was bent to the exit. The 1 cm difference between the roof bend cross-section height and drawdown cross-section height is considered as diverter. Also, cross-section dimensions are kept big in order to reduce subsidence amount necessary for siphon inlet by keeping the input speed level small, whereby, inlet bend of the siphon is eliminated; only $\alpha = 90^0$, bend is available at the outlet.

This automatic siphon is being applied with an open waterway sinuous part ($\alpha = 30^0$, $\alpha = 60^0$, $\alpha = 90^0$) and applied as ($\alpha = 0^0$) "side weir" at the flat part, speed and level measurements are done, priming and stop conditions of the siphon were determined.

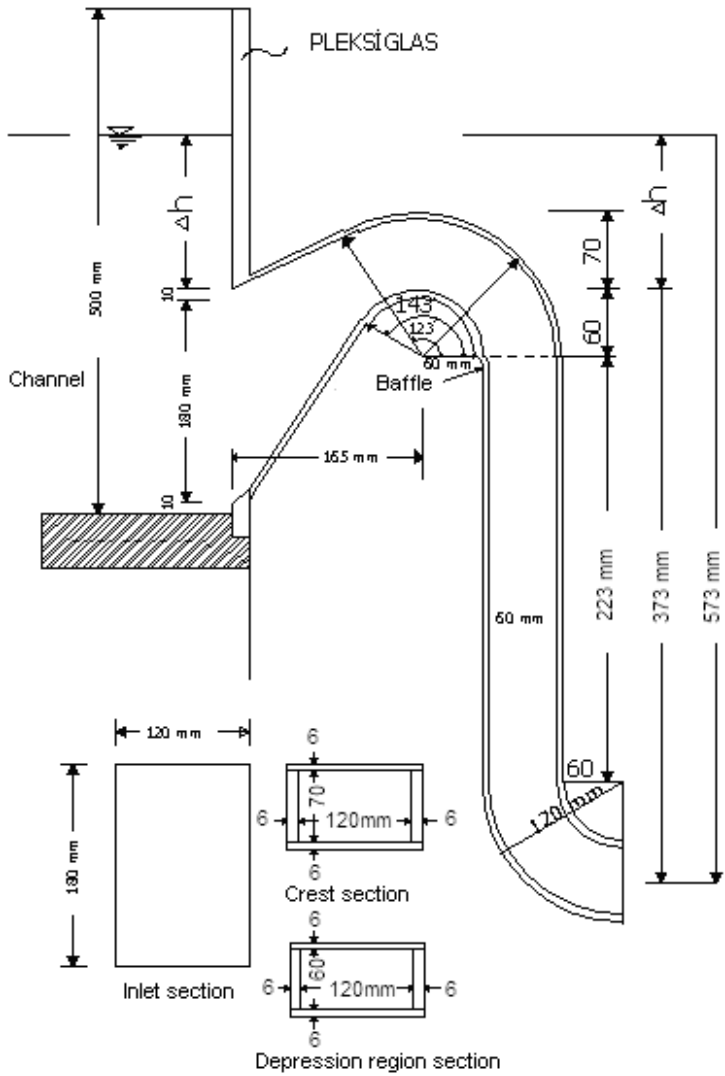

Fig. 6. Automatic siphon details

When determining the size of the model, as well as the geometric dimensions of the existing waterway and Gibson's (Gibson, Aspey & Tattersal (1930)) model scale conditions were taken into consideration as well as in classic siphon. According to the existing geometric conditions, the maximum height between the upper water level at the siphon inlet and outlet section axis is h=57.3 cm, head of water over siphon crest for this study is Δh=20 cm and inner radius of the roof bend of the siphon r_i = 6 cm.

According to these values, upon Gibson's minimum model scale conditions, roof cross-section height of the siphon should be:

$d\sqrt{h} > 47.1\ cm^{3/2}$

$d\sqrt{57.3} > 47.1\ cm^{3/2}$

$d > 6.2\ cm$

In this mode, d is taken as 7 cm. Siphon cross-section width b is determined as 12 cm by considering the width/height ratio that gives most suitable section value for cross-section of the rectangular (b/d=2 is taken as basis for cross section drawdown area).

Obtaining rectangular weir rating curve

Rectangular weir rating curve was obtained by releasing the whole flow at the main waterway to the collecting waterway. Flow rates which read from the electromagnetic flow rates are given in rating curve (Figure 7) by measuring the nappe thickness over the rectangular weir. The equation of the rectangular weir at the end of the collecting waterway was being obtained at the figure below.

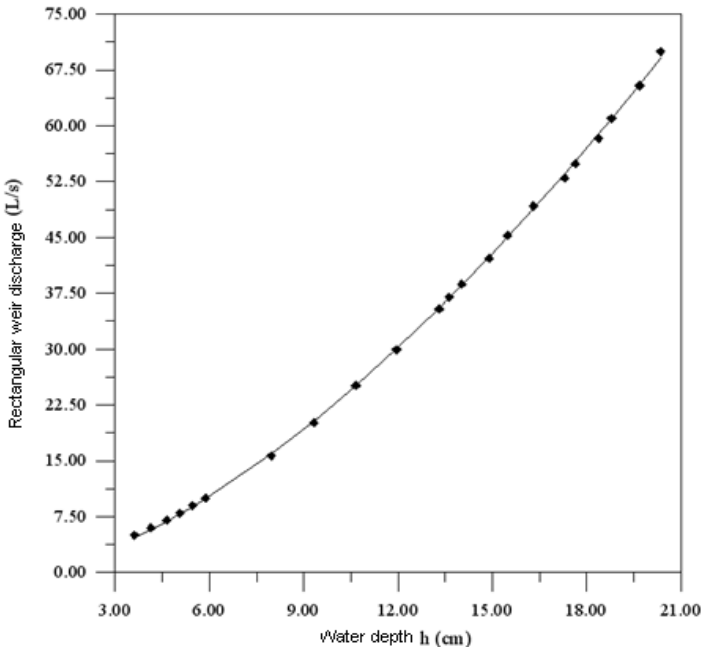

Fig. 7. Rectangular weir rating curve

Determination of the priming and stop conditions of the siphon at the experiment waterway

In an automatic siphon in the form of side weir; in order to determine "priming and depriming" conditions', an automatic model siphon was placed to curved parts of the waterway respectively as 0^0 (flat part) and 30^0 ‘of 60^0 of 90^0 as a side weir vertical to

the flow direction of the waterway, then speed and level experiments were made at the various stages of the water level adjust cap at various flow rates and some of the issues have been identified (Figure 8a , Figure 8b , Figure 9a & Figure 9b).

It is determined that at the automatic siphon used in the experiments, the ratio of priming height which varies to flow speed of the waterway to floor section have values between 4/7 and 6.5/7.

The vortex which is originated from the siphon inlet through the headwater, and the water level at the waterway is slightly lowered when siphon is priming and air enters into the siphon. The intake air is spread within the siphon. This event shows /1} the negative effects of the secondary and accordingly helicoidal flow during the stopping as well as priming. As a result, vibration intensity is further increased since the air which entered into the siphon from the inlet cannot be uniformly distributed.

It is observed that siphon starts to work when the water level in the waterway reaches the h = 21.8 cm. Full-siphon flow is monitored when the water level is = 25.7 cm. Low amount of air enters the siphon between the values h= 21.8 and h= 25.7 cm.

Fig. 8a. The beginning of priming siphon

Fig. 8b. Priming siphon

Fig. 9a. Full siphonic discharge

Fig. 9b. Full siphonic discharge

RESULTS AND DISCUSSION

Speed distribution profiles along the side weir

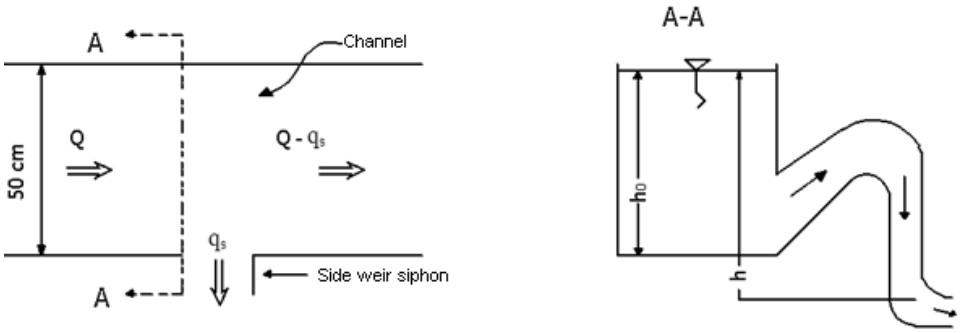

Fig. 10. The plan and cross-section of the channel and siphon

At the A-A axis, Froude numbers and flow rate coefficients are calculated at the siphon weir inlet, which can also be seen from Figure 10 Siphon weir flow rates are being found by substituting the measured water levels at the end of the collecting waterway (Figure 3) into formula 4.1 given in the rectangular weir rating curve.

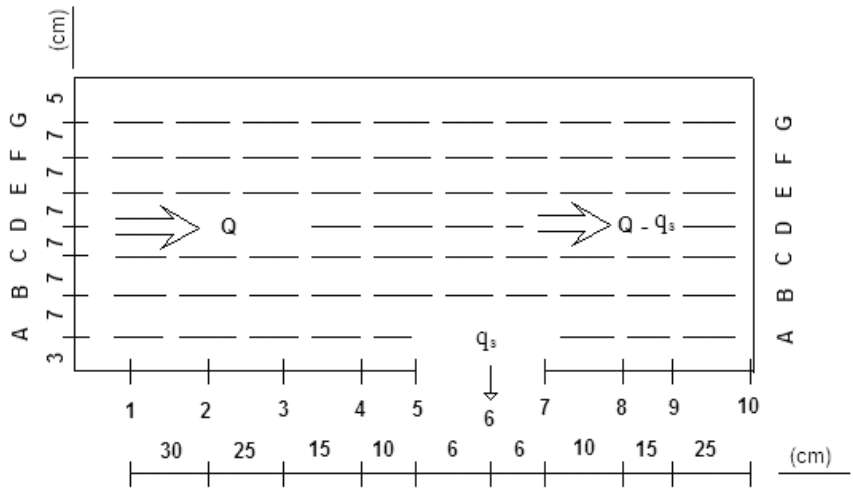

Fig. 11. Siphon in the form of the side weir, the speed distributions at the waterway

Figure 11 is the plan of the main channel. The horizontal space between 5 to 7 is siphon spillway. Vertical letters and horizontal numbers show measurement points. Measurements during the determination of the speed distributions (as seen in Figure 11) are done over profile in Figure 11, as shown in seven different measurements for each weir axis (AA, BB, CC, DD, EE, FF and GG), and were 10 different points on each axis (figures 1 to 10 for each axis up to 10 different chart shown). After placing the automatic siphon to the base of the waterway, measurements were made with Micromuline (0.02-5 m/s). Micromulins were mounted on the moving level and speed measurement car and measurements were done in the direction of the flow. Measurements were made at intervals of 5 cm from waterway base (0.5 cm) to the surface of the water. The first axis (A-A axis) is at a distance of 3 cms from the weir.

Measurements were done at two different flow rates; 30 L/h and 100 L/h. Low speeds were measured at the 30 L/h flow rate and high speeds were measured at the 100 L/h by having the adjust cap opened.

Measurements were first done at the curved parts, i.e. weirs of 30 ^{0,} 60 ^{0} and 90 ^{0}, then at the flat parts, i.e. 0 ^{0} .The results are shown in the following ways as dimensionless. Then, their explanations were made.

In the drawings: z value indicates the height of the water where the measurement is done from the waterway base, h value indicates the total water level, v value indicates the speed of the point where measurement was done, v_m value indicates the maximum speed value of the point where measurement was done.

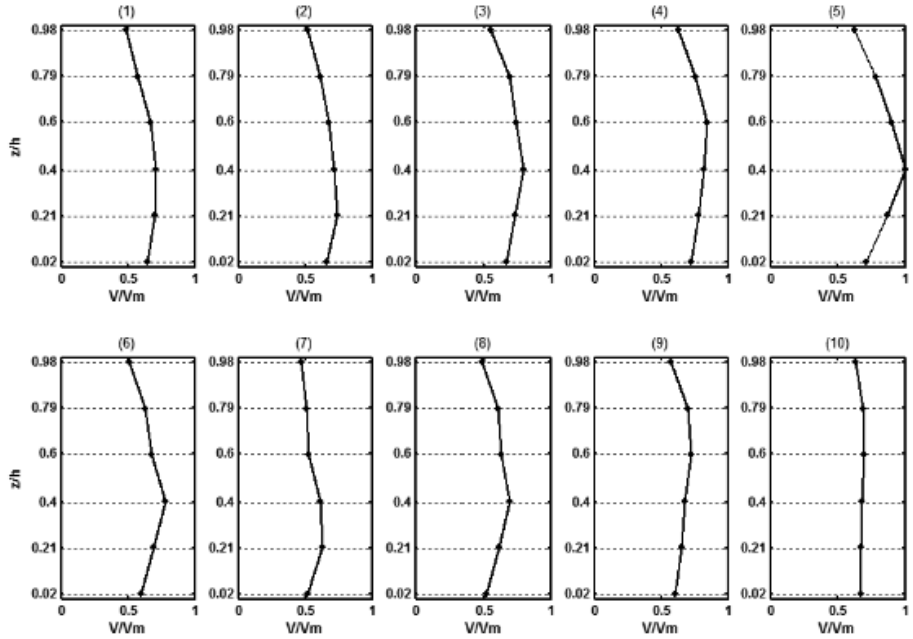

30 ^{0,} Q = 100 l / h

AA axis

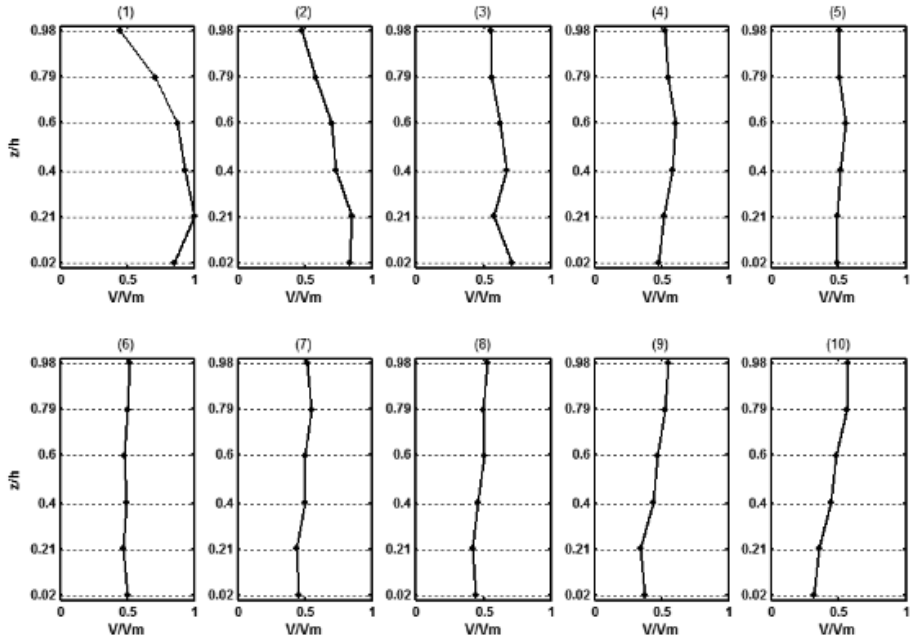

30 ^{0}, Q = 100 L/h

G-G axis

Fig. 12. Tangential speed distributions in case of active spill of the flow rate of Q = 100L/h from the α= 30 ^{0} side weir

The highest speeds measured in the weirs are being formed in the A-A axis, the section closet to siphon weir. The A-A axis is influenced too much, because the main waterway shrinks the water very quickly due its affinity to the siphon weir. The minimum speeds were formed in the G-G axis, the axis most distant to the siphon weir. The effect of siphon weir on the main waterway is the minimum since the G-G axis is the most distant axis to the siphon weir. Maximum speeds measured only in flat waterway with Q = 100 L/h are formed at B-B, C-C and D-D axis. Since the flow and speed is too much, the effect of the siphon weir on main waterway is being decreased and the biggest speeds are being formed around the middle axis of the waterway.

The highest speeds on A-axis are being measured in the point 5, in the inlet of the siphon weir during the speed measurement made with low speeds in $\alpha = 30^0$ weir, Q = 30 l/h flow. Dead spots were formed at the G-G axis, points 9 and 10; in short, the speed was measured as zero. In general, speeds are low at the bottom of waterway, high at the middle parts and again low towards the surface. The highest speed is measured again at the point 5 of the A-A axis in the measurements done at high speeds with Q = 100 L/s flow rate. However it is measured that speeds are generally low at the base, high at the middle parts and again low towards the surface; it is observed that F-F and G-G axis are increased from the base to the surface at the points 8, 9 and 10.

The highest speeds on A-A axis are being measured at the points 5 and 6, in the inlet of the siphon weir during the speed measurement made with low speeds in $\alpha = 60^0$ weir, Q = 30 l/h flow. Speeds were dramatically decreased at the points 6,7,8,9 and 10 of the G-G axis towards the surface. The highest speed is measured again at the point 5 of the A-A axis in the measurements done at high speeds with Q = 100 L/s flow rate. Minimum speeds are measured at the middle parts of the water level (at 15.5cm) of the waterway between the points 5 and 10 of CC, DD, EE, FF and GG axis. Here, high-speed channel bottom, and then decreases from the bottom section to the surface again until rising to 15.5 cm.

The highest speeds on A-A axis are being measured at point 5, in the inlet of the siphon weir during the speed measurement made with low speeds in $\alpha = 90^0$ weir, Q = 30 l/h flow. Dead spots occurred at the points of 9 and 10 at the G-G axis. In general, speeds are low at the waterway base, middle at the middle parts and again low towards the surface. The highest speed is measured again at point 5 of the A-A axis in the measurements done at high speeds with Q = 100 L / s flow rate. Here, however it is not as clear as it was at $\alpha = 60^0$, at some point, speeds are high at the base, then decreasing till 15.5 cm from the base and then increase again towards the surface.

The highest speeds on A-A axis are being measured at point 5, in the inlet of the siphon weir during the speed measurement made with low speeds in $\alpha = 0^0$ ' weir, Q = 30 l/h flow. Unlike the curved weirs, at this weir, it is measured that the speeds are lowered a bit more at the surface and very small values are measured at the points 8 and 9 of the base at the B-B, C-C and D-D axis. Speeds were decreased dramatically at the points 9 and 10 at the G-G axis. Q = 100 L / s flow velocity measurements made at high speeds, are measured at the point 2 of the B-B, C-C and D-D axis as distinct from the weirs at the curves. Here, the values are measured as high at the base, middle at the low, and high values at the surface. Unlike the curved weirs, this weir has speeds lowering towards the surface significantly and takes minimum value.

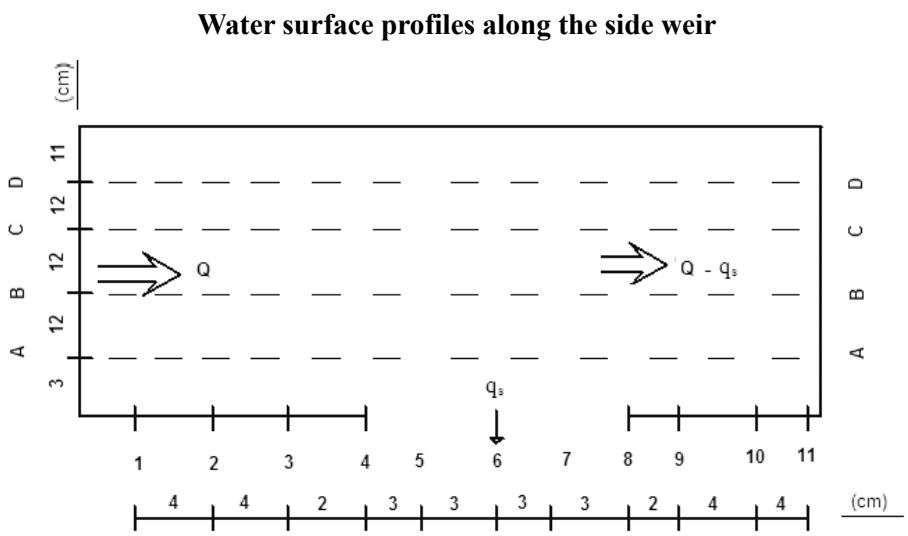

Fig. 13. Siphon in the form of side weir, waterway water surface profiles

Figure 13. is the plan of the main channel. The horizontal space between 4 to 8, is siphon spillway. Vertical letters and horizontal numbers show measurement points. While determination of water surface profiles, measurements are done on 4 different axis (A-A, B-B, C-C and D-D) and over 11 points on each axis for each weir as seen in Figure 13. Level measurements began from a distance of 3 cm from the weir. These measurements were made by 0.01mm precision electronic limn meters. Limn meters were made by mounting over the moving level and speed measurement car. Fluctuations occurred in some angles and flows during the level measurements. In order to avoid these fluctuations, wave breakers are being used, so ease of measurement was achieved.

Measurements are done firstly at the curved parts, that is $30^{0,}$ 60^{0} and 90^{0} of weirs and then at the 0^{0} flat part. These measurements are all done while the water level caps sealed in all weirs, in 20 L/s flows (Figure 14); and when the flow is being increased, measurements are done as the adjustment caps gradually being opened. In other words, measurements are being done first by opening the water level adjustment cap by 1 step (about 3 cm) at the 25L/s. Then, level measurements are done after opening the water level adjustment cap by 2 steps (lowering the water level). As the flow increases (as the water level in the waterway increases), level measurements were continued by gradually opening the water level adjustment cap. Water surface profiles as the result of level measurements are demonstrated in the following figures) Figure 14.

All numbers, both horizontal and vertical in the figures are in cms. The vertical numbers indicate the main waterway height, horizontal numbers indicate the siphon weir and, upstream and downstream height parts of the siphon *'s indicate the water surface.

h (cm)

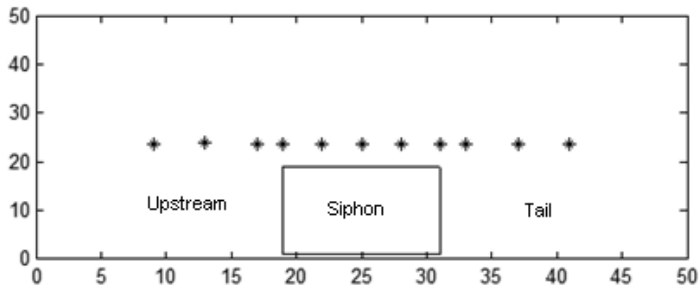

(Cm)

$30^{0,}$ AA-axis, Q = 20 L / h, $F_r = 0.1123$

h (cm)

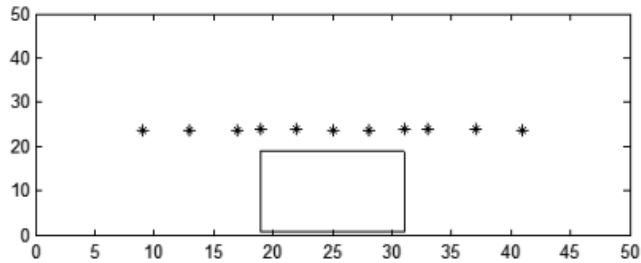

$30^{0,}$ B-B axis, Q = 20 L / h, $F_r = 0.1103$

h (cm)

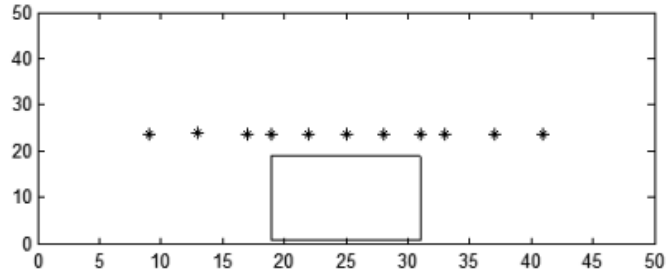

30 ^{0,} C-C Axis, Q = 20 L / h, F_r = 0.1106

h (cm)

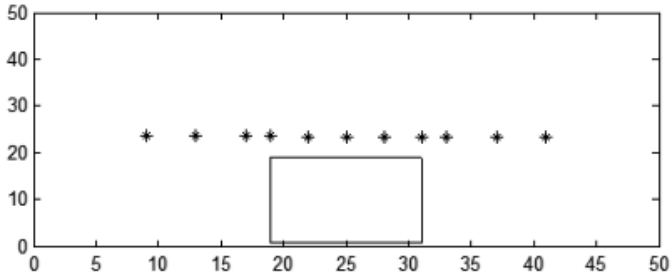

30 ^{0,} D-D axis, Q = 20 L / h, F_r = 0.1123

Fig. 14. Water surface profiles gained along the side weir threshold at the $\alpha = 30^0$, Q = 20 L/s

The most prominent features of the level measurements are seen in the A-A axis, the axis closest to the siphon weir. In this section, there often exist a drawdown of water level at the siphon weir inlet and then rises again.

In low water levels and during the priming of the siphon, vortexes are formed at the siphon inlet when an amount of air enters the siphon. This situation continues during the priming of the siphon. In high flow rates, in the A-A axis, there exist a rise after point 5 and 6 (Figure 13) and this height continues. This event, the beginning of the rise, is monitored at point 5 at the 30^0 and 60^0 ' weirs, and point 6 at the 90^0 weir and at point 5. However, it is not as obvious as in curved region.

Determination of the flow rate coefficients of the siphon weirs

These calculations are shown in Table 3.

Table 3. Determination of the flow rate coefficients of the siphon weirs

Siphon Weir Features: 30 ^{0} Curved Waterway									
h (Cm)	Q (L / h)	h_0 (cm)	v_0 (cm / s)	F_r	h_2 (cm)	h_{nap} (Cm)	q_s (L / h)	q_t (L / h)	C_d
44.71	20th	23.71	16.85	0.1106	13650	6600	11863	21325	0556
46.70	25th	25.70	19:46	0.1225	14379	7329	13976	21794	0641
44.56	25th	23:56	21:22	0.1396	13198	6148	10616	21281	0499
55.43	30th	34.43	17:43	0.0948	14990	7940	15841	23744	0667
50.05	30th	29.05	20.65	0.1223	14283	7233	13690	22562	0607
56.09	35th	35.09	19.95	0.1063	14518	7468	14393	23885	0603
46.50	35th	25.50	27.45	0.1736	14055	7005	13021	21747	0599
59.77	40th	38.77	20.63	0.1058	14769	7719	15156	24656	0615
50.04	40th	29.04	27.55	0.1632	14379	7319	13946	22560	0618
44.13	40th	23:13	34.59	0.2296	13118	6068	10401	21185	0491
51.91	60th	30.91	38.82	0.2293	14311	7261	13773	22983	0598
52.83	75th	31.83	47.12	0.2665	14320	7270	13799	23181	0595
54.80	100	33.80	59.17	0.3240	14332	7282	13835	23609	0585

Dimension analysis show that F_r Froude number is a non-dimensional parameter affecting the $C_{d,}$ side weir flow rate coefficient, accordingly, shift between the Froude numbers is calculated at the $\alpha = 0^{0,}$ $\alpha = 30^{0,}$ $\alpha = 60^0$ and $\alpha = 90^0$ and side weir flow rate coefficients are shown in Figure 15.

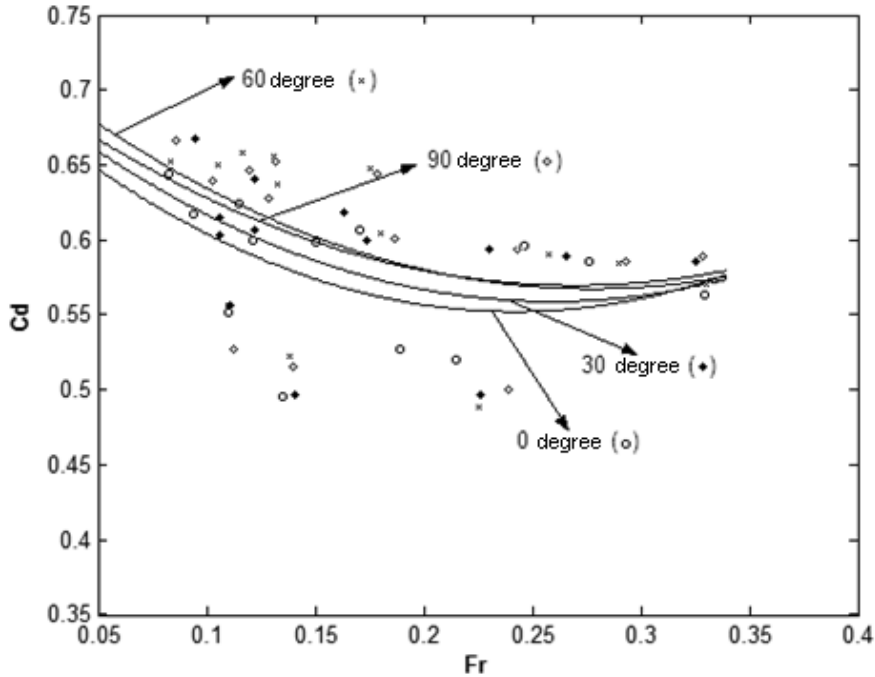

Fig. 15. Shift of Froude number in terms of side weir flow rate coefficient at the side weir regions of **α=** 0^0, $30^{0.}$ $60^{0.}$ 90^0

No big differences are observed during the comparison of the flow rate coefficients of the weirs at the curved angles of the waterway. Curve characters of 0^0, 30^0, 60^0 to 90^0 are similar to each other. All calculated flow rate are at very close values at the weirs of $\alpha = 30^0$, $\alpha = 60^0$ and $\alpha = 90^0$.

With the increase of main flow rate, it is seen that Froude numbers are also increasing. The greatest Froude numbers are found at 100 L/h flow rates in all weirs. Flow rate of 100 L/ s is the largest flow rate used in all weirs. The smallest Froude numbers are at the weirs of 30 L/h, when its adjust cap is closed.

According to these drawings, at the small F_r numbers (range from 0.05 to 0.17), i.e. the cases where flow speed is small, flow depth is big, flow rate coefficient is great in all weirs. When the F_r number is between 0.17 and 0.22, i.e. the flow depth is a bit lower, the weirs which have curve angle of 60^{0} ² and 90^{0} have the greatest C_d coefficients. In this range, flow rate coefficients at the weirs of 30 ² and especially 0^0 ‘ slightly have lower values. The biggest flow rate coefficients of the F_r number between 0.05 and 0.22 is at the weir of 60^0. This event is derived from lateral flow increasing effect due to gravitation of the maximum speed orbit to outer border after $\alpha = 45^0$ and it’s settling. At the values of F_r ‘greater than 0.20, decrease in coefficients of $C_{d.}$ are much slower. From the $F_{r.}$s value of 0.22, the weir with the curve angle of 90^0 '

has the biggest C_d coefficients. The smallest C_d coefficients of the F_r number between 0.05 and 0.32 is observed at the weir at the 0 ^{0}. Flow rate coefficients at the $\alpha = 0^0$ ' is slightly smaller than the values at the curved angles. And other results are shown in table 4.

Table 4. Biggest and smallest flow rate coefficients and Froude numbers

Weir angels	Greatest water level at the main waterway	Lowest water level	Biggest siphon weir flow rate	Smallest siphon weir flow rate	Biggest flow rate coefficient	Froude number (for biggest)	Smallest flow rate coefficient	Froude number (for smallest)
$\alpha = 30^0$	38.77 cm	23.13 cm	15,841L/h	10.401L/h	0.0948	0.667	0.2296	0.491
$\alpha = 60^0$	37.44 cm	23.33 cm	15,894L/h	9.985 L/h	0.1164	0.658	0.2266	0.476
$\alpha = 90^0$	36.90 cm	22.36 cm	16,170L/h	10.329L/h	0.0855	0.666	0.2455	0.492
$\alpha = 0^0$	37.79 cm	23.80 cm	15,744L/h	10.404L/h	0.0824	0.644	0.1353	0.486

CONCLUSIONS

In this study, the results are summarized below which occurred when; an automatic siphon is used in the different angles (30^0, 60^0 and $90^{0)}$ of a 180^0 curved open waterway, and in various flow rates (20 L/s, 25 L/s, 30 L/s, 35 L/s, 40 L/s, 60 L/s, 75 L/s, 100 L/s), in cases where used as side weir and the flow rate of side weir, Fr is analyzed from 0.0836 to 0.3381.

In the case of using an automatic siphon as a side weir in a curved waterway, parameters effecting the flow rate coefficient are determined by dimension analysis and it is found that the side weir flow rate coefficient depends on non-dimensional

$$C_d = f(\mathrm{Fr}, \frac{b}{r}, \frac{d}{h}, \theta)$$

Ratio appears to be between the flow rates spill from the siphon with the water level in the main waterway and flow rate coefficients. In addition, when the flow speed is increased, the flow rate of the siphon weir is being reduced. The reason for this is because of the change of the siphon inlet conditions and increase in the effect of the helicoidal flow intensity of the siphon.

No big difference is observed when the flow rate coefficients of the weirs at the curved angles of the waterway are compared. All calculated flow rate coefficients are at very close values at the weirs of $\alpha = 30^0$, $\alpha = 60^0$ and $\alpha = 90^0$. At the small F_r numbers (range from 0.05 to 0.17), i.e. the cases where flow speed is small, flow depth is big, and flow rate coefficient is great in all weirs. When the F_r number is between 0.17 and 0.22, i.e. the flow depth is a bit lower, the weirs which have curve angle of

60^0 and 90^0 have the greatest C_d coefficients, and especially if it is at the 30^0 and 0^0 weir C_d coefficients are at lower values. The biggest flow rate coefficients of the F_r number between 0.05 and 0.22 is at the weir of 60^0. This event is derived from lateral flow increasing effect due to gravitation of the maximum speed orbit to outer border after $\alpha = 45^0$ and its settling. At the values of F_r greater than 0.20, decrease in coefficients of C_d are much slower. From the F_r's value of 0.22, the weir with the curve angle of 90^0 ' has the biggest C_d coefficients. The smallest C_d coefficients of the F_r number between 0.05 and 0.32 is observed at the weir at the 0^0. Flow rate coefficients at the $\alpha = 0^0$ ' is slightly smaller than the values at the curved angles.

Since the air ejector water nape at the priming unit of the siphon (diverter) is asymmetric and cannot properly function (i.e. uncollision to opposing wall of the siphon within the same plane), it is observed that the priming and stoppage height of the siphon is big and the duration is long.

After full work capacity of the siphon, the water level at the waterway is being reduced at the upstream side and a superficial bulking is formed straight at the siphon inlet. This event can be clearly seen especially at the flow rates of 75 L/h and 100 L/h, in the curved region.

The highest speeds measured in the curved parts are being formed in the A-A axis, the section closest to siphon weir. The minimum speeds were formed in the G-G axis, the axis most distant to the siphon weir. However, in the flat waterway, the maximum speeds according to measurements done with Q=100 L/s occurred at the B-B, C-C and D-D axis. In addition, at the curved region of the waterway at low speeds, dead spots occurred at the surface-close parts of the points 9 and 10 of the G-G axis, which is the most distant section to siphon weir to downstream part of the siphon weir. It is seen that the effect ratio of the flow rate from the waterway cross-section is reduced by increase of the flow speed. In general, low speed channel bottom, and then again to the surface in the middle in the high and low values. However, also high values at the high values, middle in the middle speed and high at the surface are also measured. But at some high speeds, values are measured as high at the base, middle at the low, and high values at the surface.

The highest speeds on A-A axis are being measured at the point 5, in the inlet of the siphon weir during the speed measurement made with low speeds in $\alpha = 30^0$ weir, Q = 30 l/h flow. Dead spots were formed at the G-G axis, points 9 and 10. Q = 100 L / s flow velocity measurements made at high speeds. However, the maximum speed is measured at the point 5 of the axis AA. Speeds at the F-F and G-G axis are from the base towards the surface at points 8, 9 and 10. The highest speeds on A-A axis are being measured at points 5 and 6, in the inlet of the siphon weir during the speed measurement made with low speeds in 60 weir, Q = 30 l/h flow.

Speeds were dramatically decreased at points 6,7,8,9 and 10 of the G-G axis towards the surface. The highest speed is measured again at point 5 of the A-A axis in the measurements done at high speeds with Q = 100 L/s flow rate. Minimum speeds are measured at the middle parts of the water level (at 15.5cm) of the waterway between the points 5 and 10 of CC, DD, EE, FF and GG axis. Here, the values are measured as high at the base, middle at the low, and high values at the surface.

The highest speeds on A-A axis are being measured at point 5, in the inlet of the siphon weir during the speed measurement made with low speeds in $\alpha = 90^0$ ' weir, Q = 30 l/h flow. Dead spots occurred at points of 9 and 10 at the G-G axis. The highest speed is measured again at the point 5 of the A-A axis in the measurements done at high speeds with Q = 100 L/s flow rate. Speed reaches to maximum values at the DD and EE axis by increasing towards the surface.

The highest speeds on A-A axis are being measured at point 5, in the inlet of the siphon weir during the speed measurement made with low speeds in $\alpha = 0^{0}$' weir, Q = 30 l/h flow. Speeds were decreased dramatically at points 9 and 10 at the G-G axis. Unlike the weirs at the curves, the highest speed is measured at point 2 of the B-B, C-C and D-D axis in the measurements done at high speeds with Q = 100 L/s flow rate. Unlike the curved weirs, this weir has speeds lowering towards the surface significantly and takes minimum value.

REFERENCES

Agaccioglu, H. & Yuksel, Y.1998. Side-Weir flow in curved channels. Journal of Irrigation and Drainage Engineering-Asce , Vol. 124, Issue 3, pp. 163-175.

Avcı, i. 1975. Yan Savak Sifonlar. Doktora Tezi, İstanbul Teknik Üniversitesi Fen Bilimleri Enstitüsü, 207s.

Babaeyan-Koopaei,K.,Valentine,E.M. & Alan Ervin,D.2002. Case Study on Hydraulic Performance of Brent Reservoir Siphon Spillway. Journal of Hydraulic Engineering, 128, 562-567.

Babaeyan- Koopaei, K., Valentine, E.M. & Alan Ervin, D. 2001. Hydraulic Model Study Of Brent Reservoir Siphon Spillway, Proceeding of the Gongress-Interational association For Hydraulic Research, Netherlands, 504-509.

Choudhary, U.K. & Narasimhan, S. 1977. Flow in 180^0 Open Channel Rigid Boundary Bends, Journal of the Hydraulic Division, ASCE, Tec. Notes, Vol. 103., No.6, pp.651-657.

Davies, P. 1931. Correspondence on Experiments on Siphon Spillways, Proc. I.C. Engineers, Vol.231, London.

El-Khashab,A.M.M.1975. Hydraulics of Flow over Side Weirs, Ph.D. Thessis University of Southampton, England.

Erkek C. & Ağiroğlu N. 2002. Su Kaynakları Mühendisliği, Beta Basım Yayım Press, İstanbul.

Gibson, A.H. , Aspey T.H. & Tattersal, F. 1930. Experiments on Siphon Spillways, Proc. I.C.E., Part I, Vol.231, London.

Hardwick, J.D. & Grant, C,J. 1997. An Adjustable Air-regulated Siphon Spillway. Proc Instn Civ. Wat.,

Marit. And Energy, 124, 95-103.

Inglis, C.C. 1931. Correspondence on Experiments on Siphon Spillways, Proc. I.C. Engineers, Vol.231, London.

Khatsuria, R.M. 2005. Hydraulics of Spillways and Energy Dissipators. Marcel Dekker, New York, 629p.

Neary, V. S. & Odgaard, A. J. 1993. Three-dimensional flow structure at open channel diversions, Journal of Hydraulic Engineering 119(11): 1223–1230.

Skury. A. 1950. Flow Around Bends in Open Flume, Transactions, ASCE, Vol.115, pp.751-779.

Wehry, A. 1969. Increase of he Fall and Capacity of Siphon Spillways, 13 Th Congress I.A.H.R., Vol.5-1, Kyoto.

Submitted: 24/5/2014
Revised: 15/10/2014
Accepted: 23/10/2014